Temperature Dependence of O + OH at 136−377 K Using Ozone Photolysis†

Robert Robertson and Gregory P. Smith*

Molecular Physics Laboratory, SRI International, Menlo Park California 94025

Received: October 13, 2005; In Final Form: November 28, 2005

Ozone was photolyzed at 248 nm in 40 Torr nitrogen with small amounts of water or hydrogen added in a cooled or heated flow cell, to measure the O + OH rate constant at 136−377 K. Rate constant values were determined by kinetic modeling of the OH decays in excess O as monitored by laser-induced fluorescence and are in reasonable agreement with current recommendations. Results may be summarized by the expression $k = 11.2 \times 10^{-11}\ T^{-.32}\ e^{177/T}$ cm^3/molecule/s.

1. Introduction

Ozone photochemistry in the upper stratosphere and mesosphere is controlled largely by simple reactions of odd hydrogen species, HO_x. Recent observations by satellite and balloon provide atmospheric OH concentration measurements; however, model results based on this chemistry substantially overpredict these values.[1−3] A related model result is low ozone prediction. Among the most sensitive and uncertain reactions[4] are the difficult-to-measure radical−radical processes $OH + HO_2 \rightarrow H_2O + O_2$, $O + HO_2 \rightarrow OH + O_2$, and $O + OH \rightarrow H + O_2$. Proposed rate constant changes[1−3] to remove model discrepancies include decreasing $O + HO_2$ and increasing O + OH. High-power laser photolysis sources and diagnostics provide opportunities to remeasure these rate constants to greater accuracy and to endorse or restrict such proposed changes. We previously reported a new determination of the rate constant for O + OH at room temperature, using complete photolysis of ozone as the source of excess O atoms and the $O(^1D) + H_2O$ reaction to form OH monitored by laser-induced fluorescence (LIF).[5] These measurements are extended here to explore the range of atmospheric temperatures, by cooling a new photolysis flow cell to 136 or 230 K or by heating it to 377 K. Hydrogen is used as an alternate OH source to perform the lowest temperature experiments, as validated by rate constant measurements at the other temperatures.

This reaction has also received theoretical interest, since it is the equilibrium reverse of the endothermic chain branching $H + O_2$ step that is central to combustion chemistry. The reaction proceeds through the bound intermediate HO_2 species. Some recent theoretical work by Troe and colleagues[6] investigates the low-temperature regime, as well as summarizing previous work on the system. Several authors offer trajectory calculation predictions for rate constants down to low temperatures.[7−11]

Experimental rate constant results from the literature[12−19] are shown in Figure 1. Three temperature-dependent studies of the O + OH rate constant[12−14] were used to derive the NASA panel recommendation.[15] Another room temperature study[16] gives consistent results. Recommended error bars are 20−30%. However, recent low-pressure discharge/photolysis LIF measurements of OH time decays in excess O report a 30% higher rate constant value at 298 K and a slightly greater increase at lower temperature.[17] Although the NASA panel recommendation and our recent measurement favor a 298 K rate constant of 3.3 $\times 10^{-11}$ cm^3/molecule/s, a second cluster of measurements[18,19] suggests higher values of 4.2 $\times 10^{-11}$. The limited set of experiments all deal with discharge flow measurements. Here, we report photolytic determinations to help clarify the temperature dependence of this rate constant and extend measurements to a lower temperature.

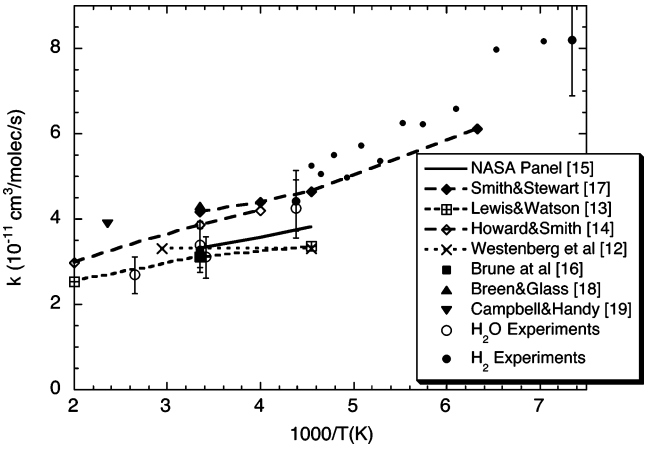

Figure 1. O + OH experimental rate constants. Error bars are one standard deviation precision.

2. Experiments

Our experimental approach uses the photochemistry employed by Marschall et al.[20] to measure $O + OH(v = 2-4)$ reaction and relaxation rate constants. A typical experiment[5] is conducted in 40 Torr nitrogen (99.99%), with metered portions of the flow picking up 50 mTorr ozone from a chilled silica trap and 100 mTorr water from a bubbler (or a similar amount of hydrogen gas flow (99.9%) is added). The O_3 concentration is determined in a separate 30 cm long cell between the calibrated mass flow meters and the photolysis apparatus by absorption of Hg penlamp radiation at 254 nm. An assumption that the water flow is at the saturated vapor pressure was confirmed by 185 nm absorption in a separate long-pass cell. A 0.20 × 0.40 cm cross-section of the cell gas is irradiated by the focused (70 cm f.l.) output of a 248 nm KrF excimer laser beam (Lambda Physik LPX-100). A measurement of laser power while a knife edge

† Part of the special issue "David M. Golden Festschrift".

* To whom correspondence should be addressed. Fax: 650-859-6196. E-mail: gregory.smith@sri.com.

10.1021/jp055863z CCC: $33.50
Published on Web 01/13/2006

is translated across the laser beam in the cell demonstrates a uniform, top-hat intensity distribution and was also used to determine the dimensions and positions of the laser beams. The irradiated dimension is larger than the previous study[5] to eliminate minor effects of diffusion on the loss rate. The excimer laser beam photolyzes almost all the O_3 in its path, and while most of the $O(^1D)$ produced in 90% yield is quenched by N_2, a small amount reacts with water or hydrogen to form the OH reactant.

After a variable delay time, a frequency-doubled Continuum Sunlite OPO laser system (pumped by the frequency tripled output of a seeded Continuum Powerlite 9010 Nd:YAG laser) measures the OH by LIF excitation of the A−X (1,0) $Q_1$3 or $Q_1$1 line near 282.24 nm. The OH (A−X, $\Delta v = 0$) fluorescence signal is collected by a 5 cm focal length lens and 310 nm interference filter and detected by a 1P28 photomultiplier tube (Hamamatsu) and prompt boxcar integrator (50 ns wide prompt gate, Stanford Research Systems SR250) interfaced to Labview computer software. The coaxial concentric OPO laser beam probes the center 0.03 cm diameter portion of the photolysis zone, with attenuated pulse energies of 0.2 μJ. The time delay between excimer and OPO laser pulses is determined by computer-controlled digital delay pulse generators for the excimer trigger and the OPO Nd:YAG pump's Q-switch. The time decay of the OH in excess O is largely determined by the targeted $O + OH(v = 0)$ rate constant, although some secondary processes will need to be accounted for quantitatively through kinetic modeling. Under the above experimental conditions, [O] > 20 [OH]. Runs averaged 30−100 laser shots per delay time point.

The excimer laser power is sufficient to photodissociate nearly all of the ozone. By monitoring the OH LIF signal level at a minimal delay after the excimer laser as a function of the excimer power, we generated a curve of ozone dissociation vs laser power which showed an asymptotic limit in OH signal that signifies saturation behavior. An exponential fit then suggests we obtained >98% ozone dissociation in the beam under typical operating fluences of about 40 mJ/pulse in the irradiated area, as was also seen in ref 5. The initial OH and O concentrations are then determined from the relative rates of the $O(^1D)$ reaction with the water or hydrogen in the mixture versus quenching by the nitrogen, using the NASA rate constant recommendations.[15] A 90% yield of $O(^1D)$ is assumed from the 248 nm O_3 photolysis. At the typical gas flow and operating rate of 10 Hz, the entire photolysis cell gas sample is replaced every laser shot. Ozone concentrations are measured directly in the flow before the photolysis cell. Then the initial O concentrations are determined, assuming 98% photodissociation.

A simple pseudo-first-order analysis of the OH decay rates vs O atom concentration at room temperature typically yields rate constant values 15% lower than the NASA recommendation[15] (with water), largely because secondary processes must also be accounted for at all concentrations investigated. These complications are not readily apparent in the pseudo-first-order decay plot, from a nonzero intercept or any curvature or baseline. The additional processes to consider include: the formation of $OH(v = 1 \text{ or } 2)$ in the $O(^1D) + H_2O$ reaction, which is then collisionally relaxed to $OH(v = 0)$ by O, H_2O, or N_2 (or reacts with O), the formation of $OH(v = 1-4)$ in the $O(^1D) + H_2$ reaction, the diffusion of O and OH from the probed region and diffusion of O_3 back in, the regeneration of OH by the reaction of the H atom product with O_3, and the removal of a small fraction of the initial O concentration by the reaction during the decay. We will account for such effects by including these kinetic processes in a model of each experimental $OH(v = 0)$ decay, and we minimize the size of the interferences by photodissociating as large a fraction of the O_3 as possible, choosing favorable experimental gas conditions, probing the center area of the photodissociation zone, and selecting the most sensitive and uncontaminated portion of the OH decay for the determination (typically an exponential from 80% to 20% of the OH peak). In addition, pressure, O atom (O_3), and OH concentrations and source gas (water or hydrogen) were varied. The ranges of conditions are listed in Table 1. No trends of different rate constant values were observed for these variables; differences were under 20% and not systematic.

TABLE 1: Range of Experimental Conditions

variable	range	typical
pressure (Torr)	20−60	40
ozone (O) (mTorr)	10−80	40
H_2O (mTorr)	10−120	33
H_2 (mTorr)	100−800	200
OH_o (ppm)	3−160	20

A new temperature-controlled apparatus was constructed for the present experiments, replacing the octagonal large-volume cell used previously.[5,20] The inner cell consists of 2 crossed 1 cm inside diameter, 20 cm length thick-walled aluminum tubes. One functions to conduct the flowing gases at the cell temperature, and the other serves as the axis of the photolysis and detection laser beams and is equipped with Brewster angle windows. This cross-tube is suspended inside an evacuated chamber and connected to a temperature bath reservoir containing a dry ice−propanol slush or liquid nitrogen. The exterior chamber also contains concentric widows to admit counter-propagating photolysis and LIF laser beams. The interior cell also has an electrical resistance cartridge heater to conduct rate measurements at higher temperatures.

The temperatures were measured by a thermocouple suspended in the gas flow within the photolysis cell. Values of 377, 228, and 136 K were obtained for the three heating cartridge and reservoir conditions. The temperature determinations of 298, 377, and 228 K were confirmed by LIF temperature scans on OH in the cell using the various rotational lines, within 10 K precision. A series of measurements was also taken at values between the two stable low-temperature baths, while the cell was cooling or warming up. The deposition of excess energy in the ozone photolysis can also cause some heating of the region of the kinetics observations. This is derived from the extra photon energy above that required for photolysis to specific products, the relaxation of vibrationally excited O_2 formed in 10% yield from ozone, and the quenching of $O(^1D)$ formed in 90% yield. Maximum amounts can be computed for the temperature jumps, and these average 8 K for the water experiments and 9 K for hydrogen. Potential rate constant increases would be 3% due to resulting density decreases. Without evidence from the LIF scans of any significant temperature increases, we made no temperature corrections for this small possible effect in the modeling and the current report.

3. Results and Analysis

A typical experimental data set and model fitting result is shown in Figure 2, for a run using hydrogen as the OH source, at room temperature. Modeling calculations with various values of the O + OH rate constant were performed with the Sandia Chemkin code Senkin,[21] using the HO_x kinetics given by the NASA panel evaluation.[15] The OH vibrational states and collisional relaxation are explicitly included up to $v = 8$. We

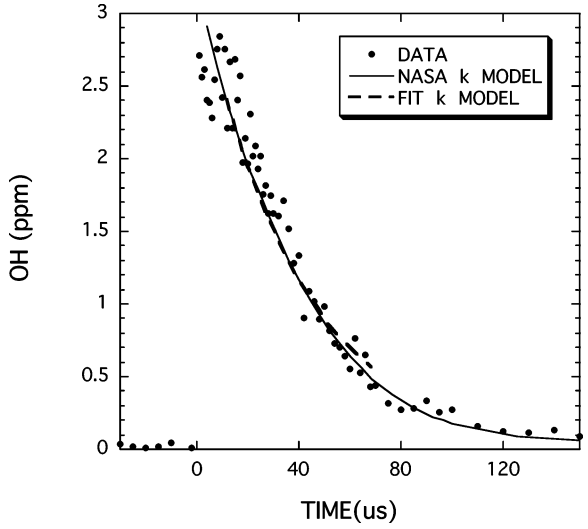

Figure 2. OH decay in an H_2 experiment (45 mTorr O_3, 0.21 Torr H_2 in N_2 at 41 Torr 298 K). The *Y* axis scale is from the model.

have assumed that the O + OH → H + O_2 reaction rate constant is independent of vibrational level. We assign any increase observed for OH(v) + O to vibrational relaxation. Literature values were taken for the OH product level branching for the O(^{1}D) + H_2O,[23] O(^{1}D) + H_2,[23] and H + O_3 reactions.[20,24] OH vibrational relaxation is mainly accomplished by collisions with O atoms and water when present. For OH(v) + O → OH(v − 1) + O vibrational relaxation, we use the difference between the total loss rate constant of 4.9×10^{-11} cm^3/molecule/s measured for 298 K at SRI[20] for OH($v = 2$) (and 11.5, 7.3, and $\sim 4 \times 10^{-11}$ for $v = 4$, 3, and 1) and the NASA $v = 0$ reaction rate constant (i.e., 1.6×10^{-11} for the $v = 2$ relaxation). The $v = 1$ value is an interpolation, and those for $v = 3$ and 4 are from preliminary measurements. A more recent value for $v = 4$ is 13% faster. The same temperature dependence ($E/R = -238$ K) was assigned to all these O atom reaction and relaxation rate constants. Rate constants measured for $v = 1$ and 2 relaxation in water[25] have been scaled by v for higher OH levels, and the upper limits determined for nitrogen[26,27] were used for relaxation by N_2 (generally insignificant). Finally, an approximate model for diffusion of O, OH, and O_3 was included by adding an exponential term for loss or gain, with time constants computed using the diffusion constants in N_2 from the Sandia transport code[28] and an approximate distance of 0.135 cm, given by the difference between the photolysis and probe laser radii. This process is negligible for the larger distances and short time decays recorded in most of the present experiments, compared to some of the runs of ref 5. Table 2 lists the rate parameters in the model to which the OH decay is sensitive, according to the sensitivity analysis also provided by the Senkin code and discussed later. The full model is listed in the Supporting Information.

For each experiment, a rate constant for O + OH was determined by first fitting the OH time decay to a single exponential over a limited decay range. For the run illustrated in Figure 2, this is from 80% to 20% of the maximum OH signal and produces a line identical to the dashed one shown with a decay time of 39 μs. Model runs, as described above, are then computed to match this decay over its fitting range by varying the O + OH rate constant—in this case giving $k = 3.1 \times 10^{-11}$ cm^3/molecule/s and the dashed line. The model O + OH(v) reactive rate constants are also assigned this value. The plot shows the result from using the similar NASA-recommended value[15] of 3.3×10^{-11}, the longer solid line. It is nearly indistinguishable from the decay trace and also describes the continuing OH decline out to much longer times. The data are inconsistent with a significantly faster or slower rate constant. The new 298 K results, with either water or hydrogen as the OH source, are identical to the previous results in the old cell.[5]

Figure 3 shows an experimental result at 136 K, along with a best fit model decay that uses a rate constant of 8.4×10^{-11} cm^3/molecule/s. The rapid decay is clearly distinguishable from the model result using an Arrhenius extrapolation of the NASA recommendation[15] outside its intended temperature range, which is shown by the later solid line.

A complete analysis of the experiments shows no variation of the rate constant with experimental variables of pressure, ozone (thus O atom), or water/hydrogen (thus OH) concentration—up to high levels. The complete experimental set using water at 298 K yields a final rate constant value of $(3.41 \pm 0.27) \times 10^{-11}$ cm^3/s (1-σ). This agrees with the NASA recommendation[15] of 3.3×10^{-11} and our previous measurement[5] in the other cell of 3.17×10^{-11}. The measurement using hydrogen as the OH source gave a consistent value of 3.27×10^{-11} , which validates this alternative source. Hydrogen is required to reach the lower temperatures where water has no significant vapor pressure. The considerably higher production of vibrationally excited OH for this source[23] is not leading to different rate constant values. We would appear not to be greatly sensitive to this complication of increased excitation, but this issue will be explored in later modeling discussions. Our rate constant value does depend some on the modeling of the observed decay and is somewhat influenced by other chosen rates including OH(v) relaxation and reaction, as discussed in the previous paper[5] and a later section.

The results of the several sets of measurement runs are summarized in Table 3 and displayed on the Arrhenius plot of Figure 1. Table 4 shows the individual low-temperature determinations. A full list of other experiments using water at temperatures of 238−377 K and hydrogen at room temperature is offered in the Supporting Information. The variations (average and standard deviations) and ranges (full) shown for the data sets are similar for hydrogen or water as the OH source gas, and similar values apply at the higher or lower temperatures. The differences between the rate constants computed directly from the observed decays (using computed initial O concentrations) and those derived more accurately from the full modeling are a relatively constant and small fraction (15%) for water but larger for hydrogen experiments. The results show a slightly greater temperature dependence than the NASA evaluation,[15] but lie within the scatter of previous measurements, and have error bars (1-σ precision in Figure 1) touching the recommendation line. Our value at 228 K is only 15% higher than the recommendation. Measurements below this temperature show a larger rate of increase, confirming and slightly exceeding the only other determination, by Smith and Stewart.[17] The rate constant at 136 K is 2.6 times the room-temperature value.

Modeling Dependence. Because the rate constants determined from the measured OH decay rates depend on kinetic modeling, the model assumptions and their effects must be evaluated to determine uncertainties in our rate constant values. This can readily be examined using sensitivity analysis. Later, we will also examine the effects of making an alternate partition for OH(v) + O product channels, reaction or vibrational relaxation, which is one of the sensitive interferences.

The sensitivity coefficients computed by the Senkin code are $S_{ij}(t) = dC_i/C_i/dk_j/k_j = d \ln C_i/d \ln k_j$ and give the relative change in concentration (OH) for a relative variation in a rate constant.

TABLE 2: Sensitive Rate Parameters for OH Decay (298 K, H_2, run of Figure 2)

reaction	k (10^{-12} cm^3/s)	source, reference	S (OH, 40 μs)	S (OH, decay t)
$O(^1D) + H_2 \rightarrow OH(v) + H$	93.	15, 23	0.53	0.31
$O(^1D) + H_2 \rightarrow OH(v = 0) + H$	17.	15, 23	0.45	−0.31
$O(^1D) + N_2 \rightarrow O + N_2$	26.05	15	−1.01	−0.05
$O + OH(v = 0) \rightarrow O_2 + H$	32.	fit	−1.27	−0.96
$O + OH(v > 0) \rightarrow O_2 + H$	32.	$=k$ ($v = 0$)	−0.52	−0.72
$OH(v) + O \rightarrow OH(v - 1) + O$	13.	20	0.51	0.23
$H + O_3 \rightarrow OH(v) + O_2$	28.92	15	0	0

Since these are logarithmic quantities, the sensitivity of a decay rate, which comes from a concentration ratio, can simply be determined from a difference in sensitivity vs time. Since the reaction rate $k_r[O] = 1/\tau$ is given by $d(\ln C_{OH})/dt$, if we pick the times t_2 and t_1 at the end and start of the fit decay, the rate sensitivity is given by $\{S_j(t_1) - S_j(t_2)\}\tau/\{t_2 - t_1\}$. This decay sensitivity (for a decay rate determined from the 80% to 20% points) as well as sensitivity coefficients for OH concentration at 40 μs are given in Table 2 for the run of Figure 2. Reference 5 showed the analogous water experiment sensitivities. The sensitivity to O + OH is near unity, with only a 4% forecast shortfall in how much a model rate constant change will alter the computed OH decay rate.

While the concentration of OH is very sensitive to the ratio of rates for $O(^1D)$ reaction vs quenching, its decay is not. This is mostly because the O concentration is only slightly diminished by increasing the minority reactive branch that produces OH. Since this rate ratio is well determined, only a few percent uncertainty in our rate constant could be produced from this source. The rate constant determination is also insensitive to the transport rates, given the conditions selected for the decay rate measurements. We also see very small negative OH decay sensitivities to vibrational relaxation from higher levels of OH-($v > 4$) and the $H + O_3$ reaction, due to the almost complete photodissociation of the ozone. Even large uncertainties in these rates would not matter. A more significant model uncertainty contribution to the rate constant determination comes from the fraction of O_3 dissociation, which directly influences the O concentration as well as the amount of OH regeneration (via $H + O_3$). Modeling the same experiment with 95% dissociation increases the derived rate constant by 4%. Altering the model hydrogen or water concentration by 10% only produces a 0.2% change.

The only other significant OH decay sensitivity comes from the contribution of the $O + OH(v = 1-4)$ reaction rate, which we assumed equal to that for $v = 0$ and the $OH(v = 1-4) + O$ vibrational relaxation rate (assumed to form the $v - 1$ level).

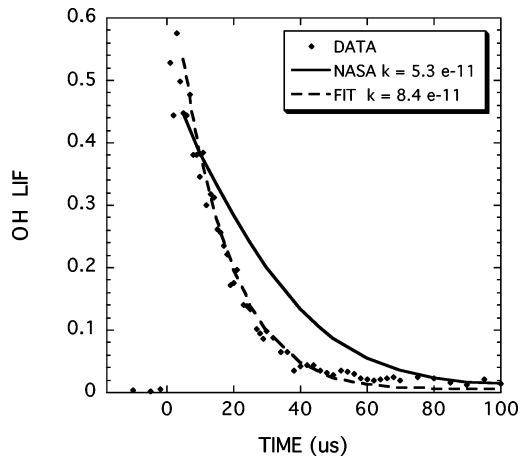

Figure 3. OH decay and model fits at 136 K. The NASA value uses an extrapolation of the expression from ref 15.

We found only small sensitivities to vibrational relaxation by N_2 or H_2, although faster relaxation by water does have a small impact on runs using this source gas as shown in ref 5. To the extent that the highly populated $OH(v = 1-4)$ from $O(^1D) + H_2$ cascades into the $OH(v = 0)$ population via vibrational relaxation by O atoms, the $OH(v = 0)$ decay is slower because of the later population additions and the real $O + OH(v = 0)$ rate constant is faster than the decay rate shows. In the earlier water experiments where $O(^1D) + H_2O$ makes mostly $OH(v = 0)$, assumptions about effects of cascading from higher vibrational levels could only affect the rate constant a few percent.[5] The H_2 source reaction makes mostly $OH(v = 1-4)$, and the sensitivity shown in Table 2 implies up to a 23% effect from these relaxation reactions on the decay. While the fact that our $O + OH$ rate constants using hydrogen and water at 298 and 228 K agree is reassuring with respect to this complication, the effects of the model assumptions for these reactions must still be explored. The basic argument, simply put, is that the $O + OH$ rate constant from the H_2 experiments agrees with previous work and the less complicated water data if and only if the surplus decay rates for $OH(v > 0)$ are modeled as a one-quantum vibrational relaxation. Otherwise, slower reactive rate constants are derived from model fits.

One extreme was assumed in the above model, that all of the measured $OH(v > 0) + O$ decay rate above the $OH(v = 0)$ value is vibrational relaxation rather than additional reaction, with the relaxation occurring in single quantum steps. The expectation from unimolecular rate theory for an exothermic barrierless reaction proceeding through a bound complex (here HO_2) is a reaction rate constant independent of reactant energy, which would justify our preferred choice. The second possible modeling limit occurs if no vibrational cascading ever affects the $OH(v = 0)$ decay, which happens if all $OH(v = 1) + O$ is reaction and no $OH(v > 1) + O$ produces $OH(v = 0)$. Therefore, some model fits were performed assuming $OH(v < 3) + O$ is entirely reaction and assigning the enhanced removal rates measured[20] for $OH(v = 3, 4)$ to one-quantum vibrational relaxation. One expects values very close to the rate constants derived from straight fits to the decay times and initial O concentrations that are shown in column 4 of Table 3. This is confirmed by the computations with the alternate model, which are only about 5% slower than the straight decay values. (The parenthetical values of column 4 in Table 3 are these alternative no-relaxation model results.) The effect of this alternate assumption would be a 15% smaller rate constant for all the water experiment sets and temperatures. Within measurement error limits, the results would still agree with the NASA recommendations[15] (perhaps with a slight low bias). The effect for the hydrogen data set, which includes the lowest temperature, is a more substantial 35% reduction in the $OH + O$ rate constant from the modeling fits (2.11 vs 3.27 at 298 K). The larger effect is a consequence of the lesser initial fraction of $OH(v = 0)$. (The correction in our first, preferred fit is thus bigger.) However, with this option the rate constants measured with hydrogen now do not agree with the measurements using water

TABLE 3: Summary of Experimental Results[a]

T (K)	gas	no. runs	decay *k*[b]	model *k*	std dev	avg dev	range	NASA[15]
293 (ref 5)	H_2O	62	2.73	3.17	.28		1.3	3.31
298	H_2O	40	2.90	3.41	.27	.21	1.4	3.29
228	H_2O	28	3.56	4.24	.35	.26	1.4	3.72
377	H_2O	22	2.27	2.69	.30	.20	1.5	3.02
298	H_2	22	1.92 (2.11)	3.27	.34	.27	1.3	3.29
228	H_2	8	2.79 (2.95)	4.36	.47	.38	1.4	3.72
136	H_2	10	5.97 (6.42)	8.53	.56	.45	1.6	(5.3)
140−220	H_2	11		6.0		N/A	N/A	(4.2)

[a] *k* in 10^{-11} cm^3/molecule/s. [b] Computed from the decay rate and initial O concentration; parenthesis values are model results without vibrational cascading.

TABLE 4: Low-Temperature O + OH Results Using Hydrogen

T (K)	*P* (Torr)	H_2 (mTorr)	O_3 (mTorr)	decay *t*[a]	decay *k*	model *k*[b]
228	37.90	220	54	17.10	2.66	4.15
	35.30	234	31	27.60	2.87	4.53
	40.30	201	74	10.80	3.08	4.56
	37.80	131	54	18.00	2.53	4.01
	37.60	539	57	18.30	2.36	3.96
	37.40	236	58	18.10	2.34	3.79
	39.8	247	31	22.77	3.44	5.22
	42.2	262	49	16.59	3.04	4.64
136	41.50	201	60	3.98	6.14	8.6
	41.30	200	60	4.34	5.63	7.76
	40.90	196	37	6.70	5.91	8.17
	40.60	198	17	15.10	5.71	8.4
	39.30	192	8.6	28.20	6.05	9.3
	41.60	402	23	10.20	6.25	8.72
	39.60	398	12	20.60	5.93	8.99
	39.10	378	39	6.43	5.85	8.23
	41.4	234	36	7.33	5.56	7.84
	38.8	219	18	12.18	6.69	9.32
142	39	243	19	14.25	5.65	8.16
153	41	256	33	8.72	5.73	7.96
164	38.5	239	17	24.34	4.27	6.59
174	40.5	251	34	12.97	4.25	6.22
181	37.5	233	15	32.39	4.02	6.26
189	39.6	246	30.4	18.43	3.64	5.35
197	37.5	233	16	36.72	3.61	5.71
203	39.8	247	32	21.29	3.21	4.97
209	37.4	232	15	43.68	3.44	5.50
215	39.7	246	31	22.86	3.27	5.06
220	37.4	232	14.4	51.93	3.17	5.25

[a] Experimental OH decay time in μs. [b] Model fit *k* in 10^{-11} cm^3/molecule/s.

and also fall below the NASA evaluation values[15] significantly. Column 4 in Table 3 illustrates this outcome clearly. Therefore, this second modeling scenario can be rejected, largely based upon the agreement seen between the two measurements and their common interpretation.

More experiments would of course be useful to resolve the O + OH(v) product yield issue, which also has some bearing on OH IR emission yields in the mesosphere. Our experiments with the chosen gas concentrations would not resolve any early rise times in OH($v = 0$) or ($v = 1$) associated with O-induced vibrational relaxation. A ~1 μs rise associated with the rotational relaxation of higher levels formed in the production reaction was observed. A short time increase in the OH($v = 2$) signal has been seen[20] that may be attributed to OH($v = 3$) + O → OH($v = 2$) + O relaxation. When better rate constants and branching ratios become available for O + OH(v), a refinement of our values can be undertaken if necessary.

Theory. Considering the atmospheric and combustion importance of the O + OH and H + O_2 reactions, and of HO_2 formation, this small, barrierless kinetic system has received much rate and quantum theory attention. There are issues of computational accuracy to deal with involving open shell

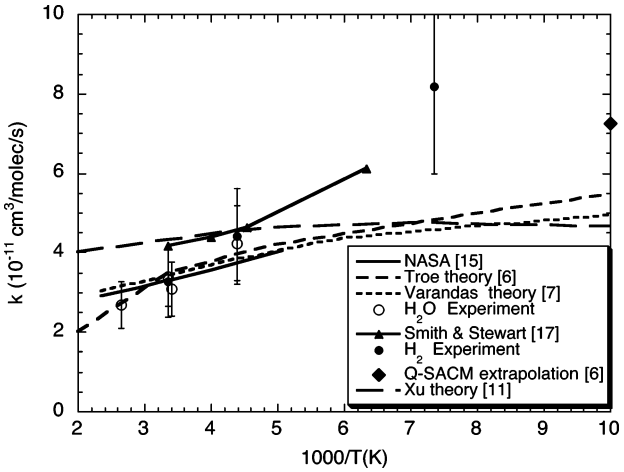

Figure 4. O + OH rate constants and theory values. Error bars are final 2-σ estimates.

fragments, treatments of angular momentum and zero-point energy, and recrossing of transition state boundaries that imply nonstatistical results. The most recent potential surface, statistical rate theory, and classical trajectory calculation results[6,7,11] provide reasonable explanations and predictions for rate constants above 200 K. Troe and co-workers[6] assign most of the observed temperature dependence to the variation in thermal population of the lowest spin−orbit state pair of reactants, O($^3P_2$) + OH($^2\Pi_{3/2}$), with little change in collision capture rate or loss by back reaction. Most theoretical calculations[6−9,11] underpredict the faster low-temperature rate constants, since the aforementioned reactant state population ratio does not increase enough (30% from 230 to 140 K). However, a limited (four channel) quantum SACM calculation performed only for temperatures below 70 K predicts faster rate constant values[6] and, if extrapolated, would account well for our 138 K results. This prediction extrapolated to 100 K and the most recent classical trajectory calculations on the Harding et al. ab initio surface,[6] the Varandas DMBE IV[7] surface, and the Xu et al.[11] ab initio surface are compared to our data and the NASA experimental evaluation line[15] in Figure 4. Other theory results are very similar. The Xu et al. theory[11] in particular predicts too little temperature dependence.

Theory can also give guidance to the issue of whether any enhanced O + OH(v) rate is due to reaction or relaxation. The most recent Troe group calculations[6] also show the O + OH collision capture cross section producing hot HO_2 equals the reaction cross section, which would seem to rule out any additional vibrational relaxation channel through the complex and also suggests no significant change in rate constant with vibrational level. A separate role in vibrational relaxation for the OH−O configuration, bound by 2 kcal/mol, is not supported by the trajectory calculations which indicate a smooth path into the HO_2 well. Nyman and Davidson[9] also find 20% or less

difference between complex formation and reaction rates, which allows for few nonreactive complex collisions, and they note the dependence of this value on how zero-point energy is treated as well.

Other calculations disagree and would allow for an OH(v) + O relaxation path equal to the reaction rate. Miller and Garrett[10] found trajectories leading to reaction on only half of the RRKM complex-forming collisions. Recently, Varandas[7] calculated reaction and vibrational relaxation rate constants for specific OH(v) levels at 255 and 210 K. He found little variation in reaction rate with vibrational level and predicted roughly equal rate constants for vibrational relaxation and reaction. This latter finding is consistent with the modest model relaxation rates for OH(v = 1 and 2) but not with the faster values measured for v = 3 and 4 [20] unless a different mechanism becomes operable. A lack of vibrational level dependence of rate constants, used in our model and found by Varandas,[7] might be expected from other experimental observations such as the finding that the high-pressure limit value for OH(v = 0) + CO → HOCO equals the OH(v = 1) + CO total removal rate constant.[29]

Conclusions

We can estimate an uncertainty in a fashion similar to the earlier room-temperature water experiment.[5] Adding in quadrature the uncertainty contributions of 9% from statistics, 8% from kinetics, 2% from ozone dissociation, and 10% from ozone concentration, we estimate a rate constant error bar (1-σ) of 16% or 22% for 2-σ statistics on each data set. An added uncertainty of up to −30% must be considered that depends on the extent of OH vibrational relaxation by O. The consistency of results obtained using water as the OH source and those with hydrogen using the vibration-independent reaction rate model suggests much less uncertainty from this issue. The 136 K rate determination is subject to greater modeling uncertainty since it could only be measured with the hydrogen system. It would thus seem prudent to include additional O + OH(v) uncertainty in the estimate. Although the statistical decay standard deviation is only 6%, we estimate from the model sensitivities of Table 2 and an added 20% remaining uncertainty for OH(v) kinetics that the model-induced uncertainty is 22%. This propagates to a 27% estimated uncertainty (2-σ) in the 136 K rate constant, $(8.5 \pm 2.3) \times 10^{-11}$ cm^3/molecule/s. New OH(v) state-specific kinetics information could reduce this error limit.

The O + OH rate constant at 298 K from three sets of measurements is confirmed to be $(3.26 \pm 0.60) \times 10^{-11}$ cm^3/s (2-σ), in agreement with the NASA evaluation of previous experimental results.[15] This value is lower than the recent low-pressure discharge/photolysis/fluorescence determination[17] and does not support any proposed large rate constant increases in models in order to better predict upper atmospheric HO_x determinations. Our complete results can be described by the expression $k = 11.2 \times 10^{-11}\ T^{-.32}\ e^{177/T}$ cm^3/s over 135−380 K. This is a slightly greater temperature dependence than the evaluation recommends, but there are no statistically significant differences.

The consistent results obtained using water or hydrogen as the OH source reactant suggest that the rapid rate constant measured using hydrogen at the lowest temperature is not highly contaminated by effects of vibrational relaxation from higher levels of OH being improperly accounted for by the model. This low-temperature value and the temperature dependence exceeds predictions of theory[6−11] and is slightly faster than expected from the prior lowest temperature measurement.[17] Additional theoretical investigations of low-temperature behavior are needed. In principle, with better thermal contacts of the cell and flow lines to the reactor, it may be possible to extend this measurement method to ∼80 K. Reports of a planned CRESU experiment to 38 K have also appeared.[30]

Acknowledgment. This work was supported by the NASA Ionospheric Thermospheric and Mesospheric Physics Program, Grant NAG5-8123. The authors thank their colleagues Drs. J. Marschall and R. A. Copeland for advice and discussions regarding the experimental protocols.

Supporting Information Available: Tables showing experimental results for H_2 and H_2O and a kinetic modeling mechanism. This material is available free of charge via the Internet at http://pubs.acs.org.

References and Notes

(1) Conway, R. R.; Summers, M. E.; Stevens, M. H.; Cardon, J. G.; Preusse, P.; Offermann, D. *Geophys. Res. Lett.* **2000**, *27*, 2613.

(2) Day, C. New measurements of hydroxyl in the middle atmosphere confound chemical models. *Physics Today*, November, 2000, pp 17−19.

(3) Jucks, K. W.; Johnson, D. G.; Chance, K. V.; Traub, W. A.; Margitan, J. J.; Ostermann, G. B.; Salawitch, R. J.; Sasano, Y. *Geophys. Res. Lett.* **1998**, *25*, 3935.

(4) Smith, G. P.; Dubey, M. K.; Kinnison, D. E.; Connell, P. S. *J. Phys. Chem.* **2001**, *105*, 1449.

(5) Robertson, R.; Smith, G. P. *Chem. Phys. Lett.* **2002**, *358*, 157.

(6) Harding, L. B.; Maergoiz, A. I.; Troe, J.; Ushakov, V. G. *J. Chem. Phys.* **2000**, *113*, 11019. Troe, J.; Ushakov, V. G. *J. Chem. Phys.* **2001**, *115*, 3621.

(7) Varandas, A. J. C. *Chem. Phys. Lett.* **2004**, *396*, 182.

(8) Varandas, A. J. C.; Marques, J. M. C. *J. Chem. Phys.* **1992**, *97*, 4050.

(9) Nyman, G.; Davidson, J. *J. Chem. Phys.* **1990**, *92*, 2415.

(10) Miller, J. A.; Garrett, B. C. *Int. J. Chem. Kinet.* **1997**, *29*, 275.

(11) Xu, C.; Xie, D.; Zhang, D. H.; Lin, S. Y.; Guo, H. *J. Chem. Phys.* **2005**, *122*, 244305.

(12) Westenberg, A. A.; de Haas, N.; Roscoe, J. M. *J. Phys. Chem.* **1970**, *74*, 3431.

(13) Lewis, R. S.; Watson, R. T. *J. Phys. Chem.* **1980**, *84*, 349.

(14) Howard, M. J.; Smith, I. W. M. *J. Chem. Soc., Faraday Trans. 2* **1981**, *77*, 997.

(15) Sander, S. P.; Friedl, R. R.; Golden, D. M.; Kurylo, M. J.; Huie, R. E.; Orkin, V. L.; Moortgat, G. K.; Ravishankara, A. R.; Kolb, C. E.; Molina, M. J.; Finlayson-Pitts, B. J. *Chemical Kinetics and Photochemical Data for Use in Stratospheric Modeling − Evaluation 14*; JPL Publication 02-25; Jet Propulsion Laboratory, California Institute of Technology: Pasadena, CA, 2003 (jpldataeval.jpl.nasa.gov).

(16) Brune, W. H.; Schwab, J. J.; Anderson, J. G. *J. Phys. Chem.* **1983**, *87*, 4503.

(17) Smith, I. W. M.; Stewart, D. W. A. *J. Chem. Soc., Faraday Trans.* **1994**, *90*, 3221.

(18) Breen, J. E.; Glass, G. P. *J. Chem. Phys.* **1970**, *52*, 1082.

(19) Campbell, I. M.; Handy, B. J. *Chem. Phys. Lett.* **1977**, *47*, 475.

(20) Marschall, J.; Kalogerakos, K. S.; Copeland, R. A. Laboratory measurements of OH(v=2) collisional deactivation by oxygen atoms; paper SA31A-21; American Geophysical Union Spring 2001 meeting, Boston, MA, 2001. Boulter, J. E.; Marschall, J.; Copeland, R. A. Manuscript in preparation, 2005.

(21) Lutz, A. E.; Kee, R. J.; Miller, J. A. *SENKIN: A Fortran Program for Predicting Homogeneous Gas-Phase Chemical Kinetics with Sensitivity Analysis*; Report SAND87-8248; Sandia National Laboratories: Albuquerque, NM, 1987.

(22) Gericke, K.-H.; Comes, F. J.; Levine, R. D. *J. Chem. Phys.* **1981**, *74*, 6106.

(23) Aker, P. M.; Sloan, J. J. *J. Chem. Phys.* **1986**, *85*, 1412. Butler, J. E.; MacDonald, R. G.; Donaldson, D. J.; Sloan, J. J. *J. Chem. Phys. Lett.* **1983**, *95*, 183.

(24) Ohoyama, H.; Kasai, T.; Yoshimura, Y.; Kimura, H.; Kuwata, K. *Chem. Phys. Lett.* **1985**, *114*, 263.

(25) Raiche, G. A.; Jeffries, J. B.; Rensberger, K. J.; Crosley, D. R. *J. Chem. Phys.* **1990**, *92*, 7258.

(26) Knutsen, K.; Dyer, M. J.; Copeland, R. A. *J. Chem. Phys.* **1996**, *104*, 5798.
(27) Dyer, M. J.; Knutsen, K.; Copeland, R. A. *J. Chem. Phys.* **1997**, *107*, 7809.
(28) Kee, R. J.; Warnatz, J.; Miller, J. A. *A Fortran Computer Code Package for the Evaluation of Gas-Phase Viscosities, Conductivities, and Diffusion Coefficients*; Report SAND83-8209; Sandia National Laboratories: Albuquerque, NM, 1983.
(29) Brunning, J.; Derbyshire, R. W.; Smith, I. W. M.; Williams, M. D. *J. Chem. Soc., Faraday Trans. 2* **1988**, *84*, 105.
(30) Smith, I. W. M. *Chem. Rev.* **2003**, *103*, 4549.